DALTON
FULL PAPER

Tricarbonylrhenium(I) halide complexes of 2-[(4*R*,6*R*)-4,6-dimethyl-1,3-dioxan-2-yl]pyridine (L^1) and 2,6-bis[(4*R*,6*R*)-4,6-dimethyl-1,3-dioxan-2-yl]pyridine (L^2): structure and solution stereodynamics

Peter J. Heard,*[a] Paul M. King[a] and Derek A. Tocher[b]

[a] *School of Biological and Chemical Sciences, Birkbeck University of London, Gordon House, 29 Gordon Square, London, UK WC1H 0PP. E-mail: p.heard@chem.bbk.ac.uk*
[b] *Department of Chemistry, University College London, Christopher Ingold Laboratories, 20 Gordon Street, London, UK WC1H 0AJ*

Received 14th February 2000, Accepted 4th April 2000
Published on the Web 11th May 2000

The non-racemic chiral ligands 2-[(4*R*,6*R*)-4,6-dimethyl-1,3-dioxan-2-yl]pyridine (L^1) and 2,6-bis[(4*R*,6*R*)-4,6-dimethyl-1,3-dioxan-2-yl]pyridine (L^2) reacted with the $[ReX(CO)_5]$ compounds (X = Cl, Br, or I) to form *fac*-$[ReX(CO)_3(L^1)]$ and *fac*-$[ReX(CO)_3(L^2)]$, respectively. The ligands co-ordinate to the metal moiety in a bidentate fashion *via* the N donor of the pyridine ring and one of the acetal O atoms. The bonding modes are confirmed by the molecular structures of $[ReI(CO)_3(L^1)]$ and $[ReBr(CO)_3(L^2)]$. There are four possible diastereoisomers, depending on the configuration at the metal and the acetal carbon atom. In the solid state $[ReI(CO)_3(L^1)]$ and $[ReBr(CO)_3(L^2)]$ exist exclusively as the *RR* and *SR* diastereoisomers, respectively. In solutions of the complexes of L^1 all four diastereoisomers are observed in varying concentrations, with the *SR* species being dominant. Only two of the four possible species are observed in solutions of the complexes of L^2, with the *SR* diastereoisomer being present in *ca*. 96% diastereomeric excess over the *RR* diastereoisomer. Above ambient temperatures both series of complexes are fluxional. A reversible *flip* of the acetal ring in the complexes $[ReX(CO)_3(L^1)]$ leads to the pair-wise exchange of diastereoisomers as a result of the formal inversion of configuration at the acetal carbon atom; the free energies of activation are in the range 78–82 kJ mol^{-1}. The ring *flip* process appears to occur *via* a pseudo seven-co-ordinate transition state, in which both O atoms of the acetal ring are loosely bound to the metal. The pendant and co-ordinated acetal rings in the complexes of L^2 are exchanged *via* the *tick-tock* mechanism; the free energies of activation are in the range 75–79 kJ mol^{-1}.

Introduction

Transition metal complexes of non-racemic C_2-symmetric chiral ligands, such as bis(oxazolines),[1] have attracted considerable attention in recent years because of their ability enantioselectively to catalyse organic transformations. Understanding the structure and bonding in these complexes is therefore important. The study of dynamic stereochemical processes in transition metal complexes can provide useful information on the metal–ligand interactions, particularly when several fluxional pathways are available.[2] We reported recently on the structure and fluxional behaviour of complexes containing the dioxolanyl ligands 2-[(4*R*,5*R*)-4,5-dimethyl-1,3-dioxolan-2-yl]-pyridine[3] and 2,6-bis[(4*R*,5*R*)-4,5-dimethyl-1,3-dioxolan-2-yl]-pyridine.[2] The question now arises as to the effects of the ring size on the structure and stereodynamics. In this paper we report on the tricarbonylhalogenorhenium(I) complexes of the non-racemic chiral dioxanyl ligands 2-[(4*R*,6*R*)-4,6-dimethyl-1,3-dioxan-2-yl]pyridine (L^1) and 2,6-bis[(4*R*,6*R*)-4,6-dimethyl-1,3-dioxan-2-yl]pyridine (L^2), namely *fac*-$[ReX(CO)_3(L^1)]$ and *fac*-$[ReX(CO)_3(L^2)]$ (X = Cl, Br, or I).

Experimental

Syntheses

Manipulations were carried out under an atmosphere of dry, oxygen-free nitrogen using standard Schlenk techniques. Solvents were dried[4] and degassed prior to use. Starting materials, purchased from Aldrich Chemical Company, were used without purification. The pentacarbonylrhenium(I) halides were synthesized using the published procedure.[5] The ligands L^1 and L^2 were synthesized from (2*R*,4*R*)-pentanediol and the appropriate pyridinecarbaldehyde, as illustrated by the example of L^1.[6] The six complexes, $[ReX(CO)_3(L)]$ (X = Cl, Br, or I; L = L^1 or L^2), were prepared as described below. Analytical data are reported in Table 1.

2-[(4*R*,6*R*)-4,6-Dimethyl-1,3-dioxan-2-yl]pyridine (L^1). 2-pyridinecarbaldehyde (10.5 mmol), (2*R*,4*R*)-pentanediol (25.0 mmol), 2,2-dimethoxypropane (30.0 mmol), and *p*-toluenesulfonic acid (*ca*. 40 mg) were refluxed for 72 hours in 30 cm^3 of toluene. The resulting toluene solution was extracted with (i) aqueous sodium carbonate (3 × 30 cm^3) and (ii) water (3 × 30 cm^3), and after drying ($MgSO_4$) was concentrated to dryness *in vacuo*. The residue was crystallised from hot hexane to yield pure L^1 in 78% yield.

Complexes $[ReX(CO)_3(L)]$ (X = Cl, Br, or I; L = L^1 or L^2). The appropriate pentacarbonylrhenium(I) halide (0.25 mmol) was refluxed for *ca*. 18 hours with a small excess of the ligand (L^1 or L^2) in 20 cm^3 of benzene. The benzene was then removed *in vacuo* and the residue crystallised by slow evaporation of a 1:1 CH_2Cl_2–hexane solution of the complex.

Physical methods

Hydrogen-1 NMR spectra were acquired on a Bruker AMX600 MHz Fourier transform spectrometer, operating at 600.13 Mz, on solutions of the samples in $CDCl_3$ or $(CDCl_2)_2$; chemical shifts are reported relative to tetramethylsilane as an internal

Table 1 Analytical data for the ligands L^1 and L^2, and the complexes $[ReX(CO)_3(L)]$ (X = Cl, Br, or I; L = L^1 or L^2)

Ligand/Complex	Yield (%)	Infrared data[a]/ cm^{-1}	Mass spectral data	Analyses[b] (%) C	H	N
L^1	78		194 $[M^+]$			
L^2	85		308 $[M^+]$			
$[ReCl(CO)_3(L^1)]$	67	1899; 1922; 2030	499 $[M^+]$; 464 $[M - Cl^+]$	33.46 (33.70)	2.99 (3.03)	2.63 (2.81)
$[ReBr(CO)_3(L^1)]$	55	1901; 1922; 2030	543 $[M^+]$; 464 $[M - Br^+]$	26.18 (30.94)[c]	3.87 (2.78)[c]	3.92 (2.58)[c]
$[ReI(CO)_3(L^1)]$	78	1901; 1927; 2030	591 $[M^+]$; 464 $[M - I^+]$	28.39 (28.48)	2.35 (2.56)	2.20 (2.37)
$[ReCl(CO)_3(L^2)]$	75	1901; 1917; 2030	613 $[M^+]$; 578 $[M - Cl^+]$	38.76 (39.18)	3.86 (4.11)	2.19 (2.29)
$[ReBr(CO)_3(L^2)]$	70	1903; 1919; 2030	657 $[M^+]$; 578 $[M - Br^+]$	36.58 (36.53)	3.63 (3.83)	2.08 (2.13)
$[ReI(CO)_3(L^2)]$	82	1906; 1919; 2030	705 $[M^+]$; 578 $[M - I^+]$	33.60 (34.10)	3.19 (3.58)	1.98 (1.99)

[a] Infrared spectra recorded in CH_2Cl_2 solution. [b] Calculated values in parentheses. [c] Poor analytical figures due to some unreacted $[ReBr(CO)_5]$ in the sample.

standard. Spectra were recorded in the temperature range 293–413 K. Probe temperatures were controlled by a standard B-VT 2000 unit, calibrated using an ethylene glycol standard, and are considered reliable to within ±1 K. Band shapes were analysed using the program gNMR.[7] Inversion-recovery experiments were carried out using the Bruker automation program INVREC. Selective inversion experiments were carried out using our program SOFTPULV, which generates the pulse sequence D1–180° UBURP256–VD–90°–free induction decay. The soft UBURP256 pulse[8] was centred on the signal to be inverted, the relaxation delay, D1, was 30 s, and the number of delays in the VD list was 24 (ranging from 10 ms to 30 s). Exchange rates were calculated from the longitudinal magnetisations using the program CIFIT.[9] Eyring activation parameters were calculated from the exchange rates; the errors quoted are those defined by Binsch and Kessler.[10] Two-dimensional exchange (EXSY) spectra were obtained using the Bruker automation program NOESYTP. A small random variation (±20 ms) in the mixing time, D8, was used to suppress any cross peaks due to scalar couplings. Typical acquisition parameters are given elsewhere.[2]

Geometric calculations were performed using the program Molden;[11] diastereoisomers were constructed using structural parameters obtained from the X-ray crystallographic determinations of the complexes. Infrared spectra were recorded in CH_2Cl_2 on a Nicolet 205 FT-IR spectrometer, operating in the region 4000–400 cm^{-1}. Mass spectrometry was carried out at the London School of Pharmacy and elemental analyses were performed at University College London.

Crystallography

Single crystals of the complexes $[ReI(CO)_3(L^1)]$ and $[ReBr(CO)_3(L^2)]$ were obtained as described above and mounted on glass fibres. Geometric and intensity data were acquired on an automatic four-circle Nicolet R3mV diffractometer, using the ω–2θ technique at 293(2) K. Three standard reflections were re-measured every 97 scans for each sample; no loss of intensity was observed. Data were corrected using routine procedures and empirical absorption corrections applied (ψ scan method). The structures were solved by direct methods and refined to convergence by least-squares (SHELXL 93).[12] The asymmetric unit of $[ReI(CO)_3(L^1)]$ contains two chemically identical, but crystallographically distinct molecules. The structure is poorly defined because of unresolved absorption problems, resulting in large estimated standard deviations on the geometric parameters and substantial 'ghost' peaks (*ca.* 6 e $Å^{-3}$) close to rhenium in the final refinement. As a consequence, the structure determination is used only to verify the connectivities in the molecule (Fig. 3); discussion of the geometric parameters is inappropriate. Crystal data, and collection and refinement parameters, are reported in Table 2, selected bond lengths and angles in Table 3.

CCDC reference number 186/1921.

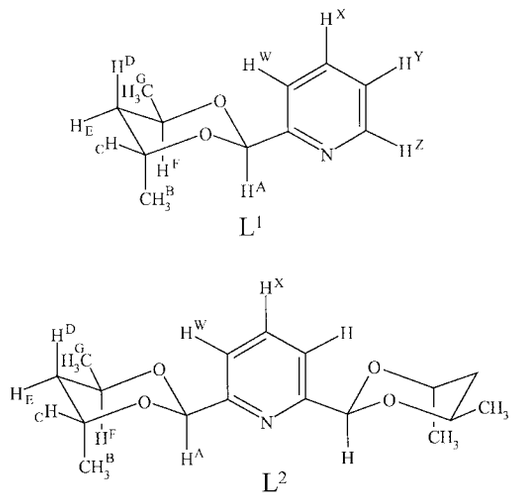

Fig. 1 The ligands L^1 and L^2, showing the hydrogen atom labelling scheme.

See http://www.rsc.org/suppdata/dt/b0/b001206h/ for crystallographic files in .cif format.

Results

Ligands

Reaction of (non-racemic) 2*R*,4*R*-pentanediol with 2-pyridinecarbaldehyde or 2,6-pyridinedicarbaldehyde in refluxing toluene yields the non-racemic chiral acetal ligands L^1 and L^2, respectively, in good yield. The ligands were characterised by mass spectrometry and NMR spectroscopy; data are reported in Tables 1 and 4, respectively. The ^1H NMR spectra of L^1 and L^2 display signals in two distinct regions, namely the acetal region (δ 1.2–6.0) and the pyridine region (δ 7.2–8.7). The acetal sub-spectra of L^1 and L^2 are similar and assignment of the signals is straightforward. The acetal hydrogen, H_A (Fig. 1), is readily identified by its low frequency chemical shift (*ca.* δ 5.9). The two-dimensional nuclear Overhauser effect (NOESY) spectra of the ligands display cross peaks between H_A and H_F, and H_A and methyl group Me_B. These cross-relaxations can only occur if the acetal ring is in a chair conformation with the pyridine ring equatorial (as shown in Fig. 1). It is noteworthy that the same conformation is present in the solid state in the complexes $[ReI(CO)_3(L^1)]$ and $[ReBr(CO)_3(L^2)]$ (see below). The unambiguous assignment of Me_B enables the signals due to the other acetal ring hydrogens to then be assigned on the basis of the scalar coupling network (COSY). The full AB_3CDEF_3 spin system was analysed using the program gNMR.[7] The pyridine-H region of L^1 displays four equally intense signals whilst that of L^2 displays two signals in a 1:2 intensity ratio; these are readily assigned on the basis of their chemical shifts and scalar couplings.[13] Hydrogen-1 NMR data are reported in Table 4.

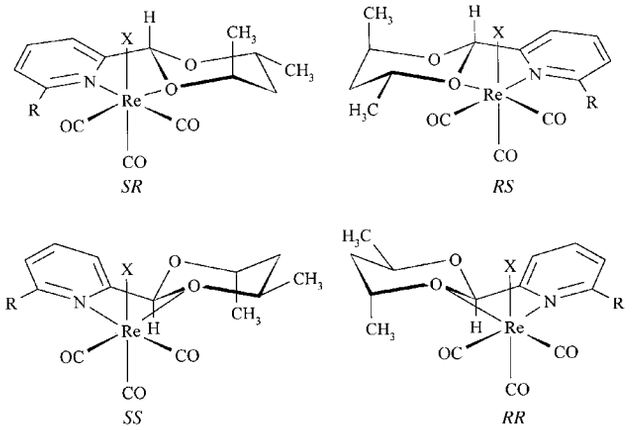

Fig. 2 The four possible diastereoisomers of the complexes [ReX(CO)$_3$(L)] (L = L^1 or L^2). L^1, R = H; L^2, R = (4*R*,6*R*)-4,6-dimethyl-1,3-dioxan-2-yl. The letters refer to the configuration at the metal and the acetal carbon atom, respectively.

Complexes

The complexes, [ReX(CO)$_3$(L)] (X = Cl, Br, or I; L = L^1 or L^2), were prepared as described above and isolated as colourless or light orange-brown, air-stable crystalline solids. Infrared spectra displayed three bands in the carbonyl stretching region, characteristic of the *fac*-octahedral [Re(CO)$_3$] moiety.[14] Elemental analyses are consistent with the formulated species except for the complex [ReBr(CO)$_3$(L^1)]. The mass spectra display low or medium intensity peaks due to the molecular ions, [M]$^+$, and a high intensity set of peaks due to the species [M − halide]$^+$. In all cases the observed and calculated isotopic patterns are consistent with the formulated species. The low analytical figures obtained for [ReBr(CO)$_3$(L^1)] arise from some unreacted [ReBr(CO)$_5$], which was observed in the mass spectrum of the compound. Analytical data are reported in Table 1.

(i) [ReX(CO)$_3$(L^1)]. Ligand L^1 co-ordinates to the *fac*-[ReX(CO)$_3$] moiety in a bidentate fashion *via* the N donor atom of the pyridine ring and one of the oxygen donor atoms of the acetal ring. The resulting complexes possess four chiral centres, namely the metal, the acetal carbon atom, and the 4- and 6-position carbon atoms of the acetal ring. The configuration at the 4- and 6-position carbon atoms of the acetal ring is *R* but that at the metal and acetal carbon atoms can be *R* or *S*. Thus there are four possible diastereoisomers, namely *RR*, *RS*, *SR*, and *SS*, depending on the configuration at the metal and the acetal carbon atom, respectively. The configuration at the metal centre is defined by viewing the molecule down the pseudo C_3 axis of symmetry (CO groups down) and assigning priorities to the three remaining ligands (halogen, oxygen, and nitrogen) according to the Cahn–Ingold–Prelog system.[15]

The four possible diastereoisomers are shown in Fig. 2. X-Ray crystallography shows clearly that the iodide complex, [ReI(CO)$_3$(L^1)], exists exclusively as the *RR* diastereoisomer in the solid state (Fig. 3), but in solutions of the complexes an equilibrium mixture of all four possible diastereoisomers is present at ambient temperature (see below). Above *ca.* 318 K, a reversible *flip* of the acetal ring leads to the exchange of pairs of diastereoisomers, namely $RR \rightleftharpoons RS$ and $SR \rightleftharpoons SS$, at a measurable rate on the NMR timescale, which was studied by dynamic NMR spectroscopy. The three complexes [ReX(CO)$_3$(L^1)] (X = Cl, Br, or I) exhibit analogous fluxional behaviour; the analysis of the problem is illustrated by [ReI(CO)$_3$(L^1)].

The ^{1}H NMR spectrum of [ReI(CO)$_3$(L^1)] (Fig. 4) displays four sets of ligand resonances of different intensities. If inversion at the co-ordinated oxygen atom of the acetal ring is assumed to be rapid on the NMR timescale, then the four sets of signals can be attributed to the four diastereoisomers depicted in Fig. 2. The assumption of rapid inversion at O is supported by *ab initio* molecular orbital calculations that indicate extremely low barriers to inversion.[16–18] To ascertain if the solid state species (*RR*) is dominant in solution, crystals of the complex were dissolved in $CDCl_3$ at 213 K and a ^{1}H NMR spectrum acquired immediately at that temperature; the spectrum displays signals due to a single species, presumably the

Table 2 X-Ray data for the complexes [ReI(CO)$_3$(L^1)] and [ReBr(CO)$_3$(L^2)]

	[ReI(CO)$_3$(L^1)]	[ReBr(CO)$_3$(L^2)]
Formula	$C_{14}H_{15}INO_5Re$	$C_{20}H_{25}BrNO_7Re$
M_r	590.37	657.52
Point group	Monoclinic	Trigonal
Space group	$P2_1$	$P3_22_1$
Mo-Kα radiation, λ/Å	0.71073	0.71073
a; *b*; *c*/Å	9.888(2); 11.569(2); 15.650(3)	14.438(2); 14.438(2); 19.673(2)
α; β; γ/°	90; 105.42(3); 90	90; 90; 120
U/Å^3	1725.8(6)	3551.5(10)
D_c/mg m^{-3}	2.272	1.845
μ/mm^{-1}	8.850	6.858
Reflections collected	3399	4700
Unique data	3208 (R_{int} = 0.0275)	2366 (R_{int} = 0.0552)
R [$I > 2\sigma(I)$]	0.0829	0.0348
$wR2$ [$I > 2\sigma(I)$]	0.2283	0.0814
R (all data)	0.0892	0.0405
$wR2$ (all data)	0.2393	0.0856
Calculated Flack parameter	0.01(3)	0.02(2)

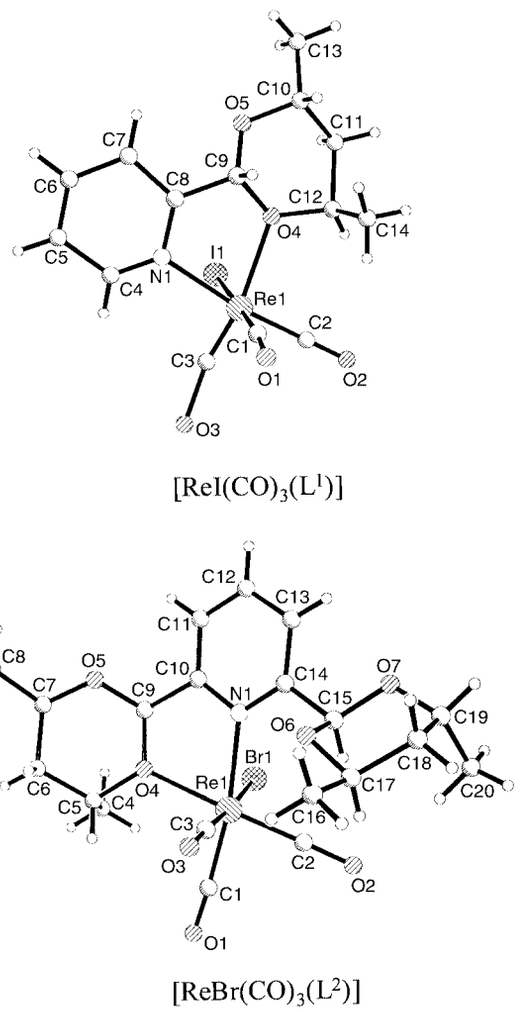

Fig. 3 The molecular structures of [ReI(CO)$_3$(L^1)] and [ReBr(CO)$_3$(L^2)], showing the atom labelling schemes.

RR diastereoisomer. On warming, signals due to the other diastereoisomers grow in; equilibration takes *ca*. 1.5 h at 303 K. Interestingly, the *RR* diastereoisomer is only the second most abundant species in the equilibrium mixture. The assignments of the three other species were made on the basis of the dynamic NMR spectra and geometric calculations. Above ambient temperature, exchange of the co-ordinated and pendant O atoms causes a formal inversion of configuration at the acetal carbon atom at a measureable rate, but not at the metal, leading to $RR \rightleftharpoons RS$ and $SR \rightleftharpoons SS$ diastereoisomerisations.[2,3] The two-dimensional exchange NMR spectrum at 328 K displays cross peaks between the *RR* diastereoisomer and the third most abundant species; this is therefore assigned as the *RS* diastereoisomer. The two remaining diastereoisomers must have the *S* configuration at the metal. Geometric calculations, based on the crystal structural data, indicate that the *SR* diastereoisomer is less hindered than the *SS* species; the more abundant of these two diastereoisomers was thus assigned as *SR* and is the dominant species in the equilibrium mixture. The EXSY spectrum also displays cross peaks due to $SR \rightleftharpoons SS$ magnetisation transfers.

The assignment of the ^{1}H NMR resonances to the different acetal ring-H and pyridine-H environments was made on the same basis as the "free" ligand assignments (see above).

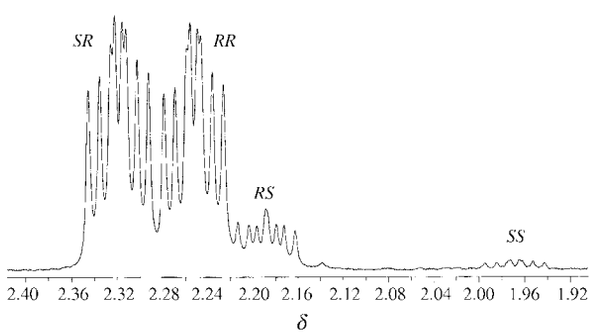

Fig. 4 Hydrogen-1 NMR spectrum of $[ReI(CO)_3(L^1)]$ in d_2-tetrachloroethane, showing the signals due to H_D of the acetal ring. See Figs. 1 and 2 for labelling.

Table 3 Selected bond lengths (Å) and angles (°) for the complex $[ReBr(CO)_3(L^2)]$

Re(1)–O(4)	2.184(7)	C(5)–O(4)	1.479(13)
Re(1)–N(1)	2.234(8)	C(9)–O(4)	1.436(12)
Re(1)–Br(1)	2.6041(12)	C(9)–O(5)	1.390(12)
C(9)–C(10)	1.528(2)	C(15)–O(6)	1.396(12)
C(14)–C(15)	1.55(2)	C(17)–O(6)	1.457(14)
N(1)–Re(1)–O(4)	72.9(2)	O(6)–C(15)–O(7)	112.1(8)
Re(1)–N(1)–C(10)	114.6(6)	C(10)–C(9)–O(4)	107.0(8)
O(4)–C(9)–O(5)	110.3(8)	O(7)–C(19)–C(18)	110.1(11)

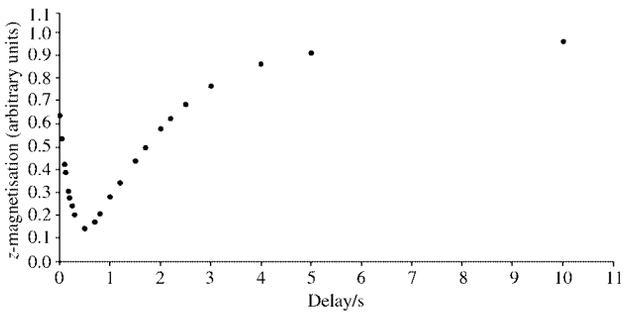

Fig. 5 Plot showing the response of the acetal-CH signal of the *RS* diastereoisomer of the complex $[ReI(CO)_3(L^1)]$ at various delay times, following the selective inversion of the corresponding signal of the *RR* diastereoisomer at 318 K. The first point is at 0.01 s. Data (not shown) were also measured at 20 and 30 s; the relative *z* magnetisation (*i.e.* intensities) at both delay times was 1.00. The rate of exchange is 0.18 s^{-1}, and the spin–lattice relaxation time is 1.28 s.

Hydrogen-1 NMR data for the three complexes $[ReX(CO)_3(L^1)]$ (X = Cl, Br, or I) are reported in Table 5; ligand scalar couplings are not affected significantly by co-ordination and are not reported.

On warming solutions of the complexes above *ca*. 328 K the bands due to the four diastereoisomers exhibit reversible broadening, indicating the onset of a fluxional process at a measurable rate on the NMR chemical shift timescale. EXSY spectra (at 328 K) display cross peaks between pairs of diastereoisomers ($RR \rightleftharpoons RS$ and $SR \rightleftharpoons SS$) as a consequence of the *formal* inversion of configuration at the acetal carbon atom. The magnetisation transfers result from exchange of the co-ordinated and pendant oxygen atoms, leading to a *flip* of the acetal ring.[2,3] No magnetisation transfers were observed between the *RR*/*RS* and *SR*/*SS* pairs, indicating that there is no inversion of configuration at Re at a measurable rate. The acetal-CH signals provide the best spectroscopic handle for the measurement of the exchange kinetics. Rates were measured in the slow and intermediate exchange regimes by selective inversion experiments[19–22] and standard band shape analysis,[23] respectively. The acetal-CH signals of the *RR* and *SR* diastereoisomers were selectively inverted at 318, 323, and 328 K (Fig. 5) and band shapes were analysed according to dynamic spin problem (I).

The dynamic NMR spectra indicate magnetisation transfers due to two rate processes, namely $SR \rightleftharpoons SS$ and $RR \rightleftharpoons RS$, in accord with the results of the EXSY. Good data for $RR \rightleftharpoons RS$ fluxion were obtained over the full temperature range, but the low concentration of the *SS* diastereoisomer frustrated accurate analysis of the $SR \rightleftharpoons SS$ process, for which only a single rate was obtained (from the initial band broadening[24] of the *SR* resonance). Spectra do not indicate the

Table 4 Hydrogen-1 NMR data[a] for ligands L^1 and L^2

L^1		L^2	
δ	Scalar couplings/Hz	δ	Scalar couplings/Hz
H_A 5.91		H_A 5.92	
H_B 1.52	J_{BC} 6.87	H_B 1.49	J_{BC} 7.05
H_C 4.51	J_{CD} 6.13; J_{CE} 1.00	H_C 4.49	J_{CD} 6.13; J_{CE} 1.10
H_D 2.04	J_{DE} 13.33; J_{DF} 11.74	H_D 2.01	J_{DE} 13.30; J_{DF} 11.50
H_E 1.47	J_{EF} 2.41	H_E 1.44	J_{EF} 2.50
H_F 4.26	J_{FG} 6.16	H_F 4.25	J_{FG} 6.15
H_G 1.31		H_G 1.27	
H_W 7.64	J_{WX} 7.90; J_{WY} 1.16; J_{WZ} 0.90	H_W 7.64	J_{WX} 7.77
H_X 7.73	J_{XY} 7.51; J_{XZ} 1.80	H_X 7.78	
H_Y 7.25	J_{YZ} 4.90		
H_Z 8.60			

[a] Recorded in $CDCl_3$ at 298 K; chemical shifts reported relative to $SiMe_4$ as an internal standard; see Fig. 1 for labelling.

Table 5 Hydrogen-1 NMR chemical shift data[a] for complexes $[ReX(CO)_3(L)]$ (X = Cl, Br or I; L = L^1 or L^2)

Complex	Diastereomer[b]	H_A	H_B	H_C	H_D	H_E	H_F	H_G	H_M	H_N	H_O	H_P	H_Q	H_R	H_S	H_W	H_X	H_Y	H_Z
$[ReCl(CO)_3(L^1)]$	*SR* (67)	6.45	1.79	4.92	2.72	1.53	4.32	1.32								7.60	7.96	7.45	8.70
	RR (26)	6.07	1.74	4.89	2.62	1.59	4.32	1.34								7.62	7.96	7.47	8.68
	RS (6)[c]	6.63	1.62	4.52	2.18		4.75	1.48								7.55			8.76
	SS (≈1)	6.11																	
$[ReBr(CO)_3(L^1)]$	*SR* (88)	6.46	1.79	4.93	2.28	1.54	4.32	1.32								7.60	7.96	7.46	8.71
	RR (9)	6.07	1.74	4.90	2.26		4.32	1.35								7.62	7.96	7.47	8.68
	RS (2)	6.64		4.52	2.19		4.75									7.56			8.76
	SS (≈1)	6.11																	
$[ReI(CO)_3(L^1)]$	*SR* (46)	6.38	1.76	4.91	2.32	1.53	4.33	1.33								7.58	7.94	7.46	8.75
	RR (45)	6.05	1.72	4.87	2.25		4.31	1.35								7.60	7.94	7.45	8.75
	RS (9)	6.60		4.53	2.19		4.74									7.54			8.80
	SS (≈1)	6.08		4.44	1.97														
$[ReCl(CO)_3(L^2)]$	*SR* (≈98)	6.53	1.86	5.07	2.21	1.54	4.32	1.30	6.39	1.51	4.53	1.94	1.46	4.47	1.24	8.04	7.97	7.58	
$[ReBr(CO)_3(L^2)]$	*SR* (≈98)	6.48	1.82	5.02	2.25	1.54	4.32	1.31	6.34	1.51	4.52	1.94	1.45	4.48	1.23	8.04	7.96	7.56	
$[ReI(CO)_3(L^2)]$	*SR* (≈98)	6.38	1.76	5.01	2.32	1.53	4.34	1.32	6.36	1.51	4.50	1.94	1.45	4.49	1.22	8.05	7.95	7.53	

[a] Spectra recorded at 298 K in $(CDCl_2)_2$; see Fig. 1 for labelling (labels A–G refer to the co-ordinated acetal ring and M–S to the corresponding signals for the unco-ordinated acetal ring of L^2); not all signals of the minor diastereoisomers are resolved. [b] Population (%) given in parentheses. [c] The assignments of H_B and H_G may be reversed.

Table 6 Eyring activation parameters[a] for complexes $[ReX(CO)_3(L)]$ (X = Cl, Br or I; L = L^1 or L^2)

Complex	Exchange process[b]	$\Delta H^{\ddagger}$/kJ mol^{-1}	$\Delta S^{\ddagger}$/J K^{-1} mol^{-1}	$\Delta G^{\ddagger}$/kJ mol^{-1}
$[ReCl(CO)_3(L^1)]$	*SR* ⟶ *SS*			≈82[c]
	RR ⟶ *RS*	83.83 (0.35)	9.88 (0.97)	80.89 (0.06)
$[ReBr(CO)_3(L^1)]$	*SR* ⟶ *SS*[d]			≈81 at 333 K
	RR ⟶ *RS*	78.56 (0.62)	−7.11 (1.75)	80.68 (0.10)
$[ReI(CO)_3(L^1)]$	*SR* ⟶ *SS*[d]			≈78 at 318 K
	RR ⟶ *RS*	77.67 (1.77)	−11.67 (5.01)	81.15 (0.28)
$[ReCl(CO)_3(L^2)]$[d]	*RS* ⟶ *SS*			≈79 at 318 K
$[ReBr(CO)_3(L^2)]$[d]	*RS* ⟶ *SS*			≈77 at 323 K
$[ReI(CO)_3(L^2)]$[d]	*RS* ⟶ *SS*			≈75 at 313 K

[a] Errors given in parentheses; $\Delta G^{\ddagger}$ reported at 298 K except[d]. [b] See text for labelling. [c] Approximate value obtained from partial band shape analysis; estimated error ±1 kJ mol^{-1}. [d] $\Delta G^{\ddagger}$ estimated from initial band broadening; estimated error ±4 kJ mol^{-1}.

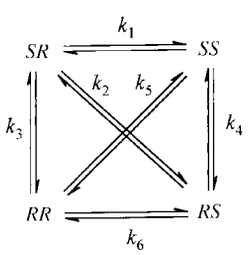

(I)

presence of any other dynamic processes (*i.e.* rates k_2, k_3, k_4 and k_5 were negligible at all temperatures). Activation parameters are reported in Table 6.

(ii) $[ReX(CO)_3(L^2)]$. Ligand L^2 also co-ordinates to the tricarbonylhalogenorhenium(I) moiety in a bidentate fashion, *via* the nitrogen donor of the pyridine ring and one of the oxygen donors of an acetal ring. The bidentate bonding mode is confirmed by the molecular structure of $[ReBr(CO)_3(L^2)]$ (Fig. 3). As for the complexes of L^1 (see above), four diastereoisomers are possible (*RS*, *RR*, *SR*, and *SS*), depending on the configuration at the metal and the acetal carbon atom of the co-ordinated acetal ring, respectively. In the solid state, the bromo complex, $[ReBr(CO)_3(L^2)]$, exists exclusively in the *SR* configuration (Fig. 3). In solution, two of the four possible diastereoisomers are observed; the dominant species is in *ca.* 96% diastereomeric excess (d.e.). Crystals of $[ReBr(CO)_3(L^2)]$ were dissolved in $CDCl_3$ at 213 K and a ^1H NMR spectrum acquired immediately at that temperature. A single species was observed with the same NMR parameters as those of the dominant species; the dominant solution-state species was thus assigned as the *SR* diastereoisomer. The minor diastereoisomer was assigned as *RR* (see below).

The bidentate mode of ligand co-ordination breaks the C_2 symmetry of the ligand, consequently the ^1H NMR spectrum of $[ReBr(CO)_3(L^2)]$ displays 14 signals in the acetal region and three signals due to the pyridine ring-H nuclides for each diastereoisomer. The assignment of the acetal signals to the pendant and co-ordinated rings was based on the co-ordination shifts, but is not unambiguous. Co-ordination of ligand L^1 (see above) causes a high frequency shift of the acetal C–H resonances; the higher frequency acetal C–H signal in $[ReBr(CO)_3(L^2)]$ was thus assigned to the co-ordinated ring. The assignments of the other acetal signals can then be made on the basis of COSY and NOESY experiments. Hydrogen-1 NMR chemical shift data for the major diastereoisomer are reported in Table 5; accurate data for the minor species were not measured because of the low concentrations and extensive overlap of signals. The scalar couplings do not vary greatly from those of the "free" ligand (Table 4) and are not reported.

Above ambient temperature the diastereoisomers undergo dynamic chemical exchange. There are three possible exchange processes (Scheme 1):[2] (i) *flip* of the co-ordinated acetal ring; (ii) exchange of the pendant and co-ordinated acetal rings *via* a *tick-tock* mechanism and; (iii) exchange of the pendant and co-ordinated acetal rings *via* a *rotation* mechanism. The *tick-tock* fluxion is readily distinguished from the others because it leads to exchange of the 3- and 5-position pyridine-H environments of the two diastereoisomers. Hydrogen-1 EXSY spectra show clearly that diastereoisomerisation is accompanied by exchange of the 3- and 5-position pyridine signals. The stereodynamics must therefore arise from the *tick-tock* exchange of the pendant and co-ordinated acetal rings. This process results in inversion of stereochemistry at the metal centre; the configuration at the

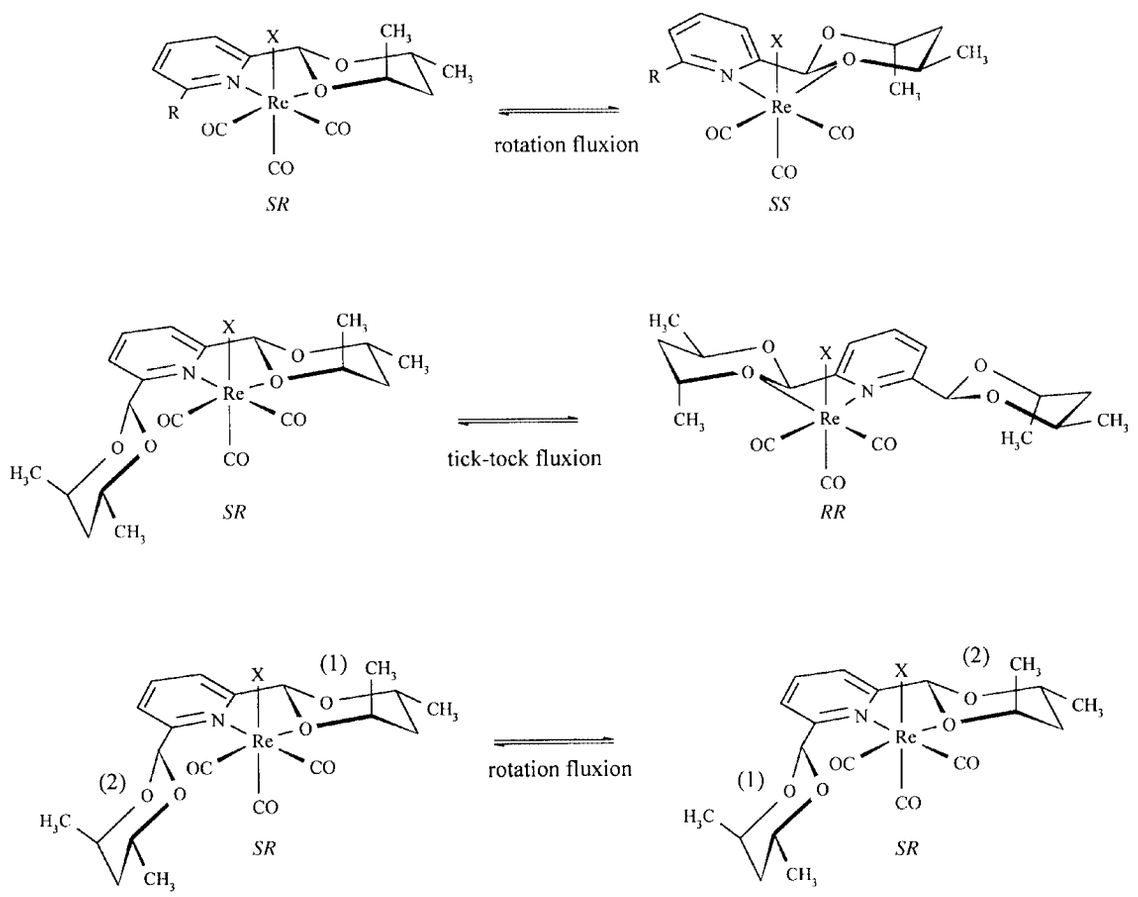

Scheme 1 The possible exchange processes in the complex $[ReX(CO)_3(L)]$ {L = L^1 or L^2 [L^1, R = H; L^2, R = (4*R*,6*R*)-4,6-dimethyl-1,3-dioxan-2-yl]}. Note that only the ring flip process is possible in the complexes of L^1. The numbers in parentheses refer to the two acetal rings, indicating the exchange process.

metal centre in the minor diastereoisomer can thus unambiguously be assigned as *R*. The configuration at the acetal carbon atom cannot be determined unambiguously. The *tick-tock* process can proceed with or without inversion at the acetal carbon. Geometric calculations based on the crystal structural data of $[ReBr(CO)_3(L^2)]$ indicate clearly that there are fewer unfavourable contacts in the *RR* diastereoisomer than the *RS*. The minor species was thus assigned as the *RR* diastereoisomer.

Hydrogen-1 NMR spectra for the complexes $[ReX(CO)_3(L^2)]$ (X = Cl, Br or I) were acquired in the temperature range 293–413 K. The observed band shape changes were fully consistent with those expected for the *tick-tock* fluxion,[2,25] but accurate quantitative data were not obtained because of the low concentration of the minor species and the extensive overlap of the signals. Approximate values for the free energies of activation were determined from the initial band broadening[24] of the pyridine 3- and 5-position hydrogen signals; data are reported in Table 6.

Discussion

(i) Complexes $[ReX(CO)_3(L^1)]$

The mono-acetal complexes, $[ReX(CO)_3(L^1)]$ (X = Cl, Br, or I), display all four of the possible diastereoisomers in solution (see above). Above ambient temperature, a pair-wise exchange of diastereoisomers, namely *SR* ⟹ *SS* and *RS* ⟹ *RR*, is observed. The observed magnetisation transfers are consistent with an acetal ring *flip* process (depicted in Scheme 1) that exchanges the co-ordinated pendant oxygen donor atoms of the acetal ligand.[2,3] No exchange was observed between the *SR*/*SS* and *RS*/*RR* pairs. The absence of exchange between all four diastereoisomers distinguishes the ring *flip* process from ligand dissociation; dissociation would lead to the averaging of all four species on the NMR timescale. The two possible mechanisms proposed previously for the acetal ring *flip* are shown in Scheme 2.[2,3] Although entropy of activation data are not very reliable, and should only be interpreted with caution, data obtained for the ring *flip* processes in the complexes of L^1, and the analogous complexes of 2,6-bis[(4*R*,5*R*)-4,5-dimethyl-1,3-dioxolan-2-yl]pyridine (L^3)[2] and 2-[(4*R*,5*R*)-4,5-dimethyl-1,3-dioxolan-2-yl]pyridine (L^4),[3] are in accord with an ordered transition state. This points clearly towards a mechanism in which both O atoms of the acetal ring are loosely bound to the metal centre [*i.e.* mechanism (i), Scheme 2].

The free energies of activation are in the range 78–82 kJ mol^{-1}, similar to the magnitudes measured previously for the complexes $[ReX(CO)_3(L^3)]$,[2] but *ca.* 6 kJ mol^{-1} lower than the magnitudes for the complexes $[ReX(CO)_3(L^4)]$.[3] The lower magnitudes of $\Delta G^{\ddagger}$ for the complexes of L^3 compared to those of L^4 were attributed to a weakening of the Re–O bond as a result of the *tick-tock* exchange of the pendant and co-ordinated acetal rings, which occurs simultaneously.[2] Geometric calculations, based on the crystal structural data for $[ReBr(CO)_3(L^1)]$ and $[ReBr(CO)_3(L^3)]$,[2] assuming a pseudo seven-co-ordinate transition state [*i.e.* mechanism (i), Scheme 2], indicate that there are fewer unfavourable steric interactions between the metal moiety and the ligand in the transition state of the complexes of L^1. The lower magnitudes of $\Delta G^{\ddagger}$ observed in the present complexes, $[ReX(CO)_3(L^1)]$, are thus thought to result from a lower transition-state energy.

(ii) Complexes $[ReX(CO)_3(L^2)]$

Only two of the four possible diastereoisomers (*RS* and *RR*) are observed in solutions of the diacetal complexes, $[ReX(CO)_3(L^2)]$ (X = Cl, Br, or I), the *RS* species being in *ca.* 96% d.e. Above ambient temperature, exchange of the pendant and

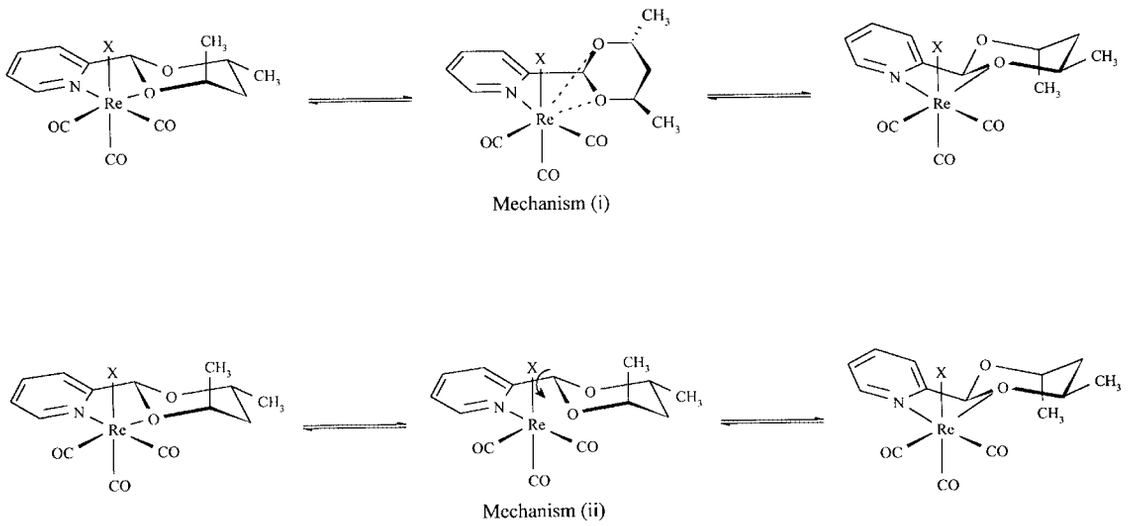

Scheme 2 Two possible mechanisms for the acetal ring *flip* fluxion.

co-ordinated acetal rings, *via* the *tick-tock* mechanism (Scheme 1), leads to the interconversion of the two diastereoisomers; the *tick-tock* mechanism is readily identified because it also leads to the exchange of the 3- and 5-position pyridine-H environments of the two species. The free energies of activation (Table 6) are in the range 75–79 kJ mol^{-1}, 3–7 kJ mol^{-1} higher than the *tick-tock* process in the analogous dioxolanyl complexes, $[ReX(CO)_3(L^3)]$ (X = Cl, Br, or I).[2] The stability of the Re–N–C–C–O chelate ring will be affected by the size of the acetal ring, and we tend to the view that the ground-state energy is likely to be lower in the dioxanyl complexes, which would account for the slightly higher free energies of activation.[26] We are currently investigating the stereodynamics in the tricarbonylrhenium(I) halide complexes of the mixed dioxolanyl/dioxanyl ligand 2-[(4*R*,6*R*)-4,6-dimethyl-1,3-dioxan-2-yl]-6-[(4*R*,5*R*)-4,5-dimethyl-1,13-dioxolan-2-yl]pyridine, to gain further insight into the effects of the acetal ring size on the energetics.

Acknowledgements

Johnson Matthey and the University of London are gratefully acknowledged for the loan of rhenium and access to the ULIRS 600 MHz NMR facility at QMW College, respectively. P. J. H. and P. M. K. acknowledge Birkbeck College for funding.

References

1 A. K. Ghosh, P. Mathivanan and J. Cappiello, *Tetrahedron Asymmetry*, 1998, **9**, 1.
2 P. J. Heard, P. M. King, A. D. Bain, P. Hazendonk and D. A. Tocher, *J. Chem. Soc.*, *Dalton Trans.*, 1999, 4495. Note the title ligand is incorrectly named as a dioxanyl in this paper. The correct ligand name is 2,6-bis[(4*R*,5*R*)-4,5-dimethyl-1,3-dioxolan-2-yl]-pyridine.
3 P. J. Heard, A. D. Bain and P. Hazendonk, *Can. J. Chem.*, 1999, **77**, 1707. Note the title ligand is incorrectly named as a dioxanyl in this paper. The correct ligand name is 2-[(4*R*,5*R*)-4,5-dimethyl-1,3-dioxolan-2-yl]pyridine.
4 D. D. Perrin and W. L. F. Armarego, *Purification of Laboratory Chemicals*, Pergamon, Oxford, 1988.
5 P. Schmidt, W. C. Trogler and F. Basolo, *Inorg. Synth.*, 1979, **28**, 160.
6 F. A. Meskens, *Syntheses*, 1981, 501.
7 gNMR v4.1.0, Cherwell Scientific Limited, Oxford, 1999.
8 H. Geen and R. Freeman, *J. Magn. Reson.*, 1991, **93**, 93.
9 A. D. Bain and J. A. Cramer, *J. Magn. Reson.*, 1996, **118**, 21.
10 G. Binsch and H. Kessler, *Angew. Chem.*, *Int. Ed. Engl.*, 1980, **19**, 411.
11 G. Schaftenaar, Molden v3.6, CAOS/CAMM, University of Nijmegen, 1999.
12 G. M. Sheldrick, SHELXL 93, University of Göttingen, 1993.
13 E. W. Abel, P. J. Heard, K. Kite, K. G. Orrell and A. F. Psaila, *J. Chem. Soc.*, *Dalton Trans.*, 1995, 1233.
14 D. A. Edwards and J. Marshalsea, *J. Organomet. Chem.*, 1977, **131**, 73.
15 E. L. Eliel and S. H. Wilen, *Stereochemistry of Organic Compounds*, Wiley, New York, 1994.
16 W. Cherry and N. Epiotis, *J. Am. Chem. Soc.*, 1976, **98**, 1135.
17 R. W. F. Bader, J. R. Cheeseman, K. E. Laidig, K. B. Wiberg and C. Breneman, *J. Am. Chem. Soc.*, 1990, **112**, 6530.
18 P. J. Heard, unpublished work, 1999.
19 A. D. Bain and J. A. Cramer, *J. Phys. Chem.*, 1993, **97**, 2884.
20 A. D. Bain and J. A. Cramer, *J. Magn. Reson.*, *Ser. A*, 1993, **103**, 217.
21 S. Forsen and R. A. Hoffman, *J. Chem. Phys.*, 1963, **39**, 2892.
22 R. E. Hoffman and S. Forsen, *Prog. Nucl. Magn. Reson. Spectrosc.*, 1966, **1**, 15.
23 J. Sandström, *Dynamic NMR Spectroscopy*, Academic Press, New York, 1992.
24 J. W. Faller, *Encyclopaedia of Inorganic Chemistry*, ed. R. B. King, Wiley, New York, 1994, vol. 5, p. 3914.
25 K. G. Orrell, *Annu. Rep. N.M.R. Spectrosc.*, 1999, **37**, 1, and references therein.
26 The lowering of the transition-state energy for the ring *flip* process must be more than sufficient to offset the (anticipated) lower ground-state energy in the complexes of L^1.